ISSN 1064-2307, Journal of Computer and Systems Sciences International, 2019, Vol. 58, No. 5, pp. 774–785. © Pleiades Publishing, Ltd., 2019.
Russian Text © The Author(s), 2019, published in Izvestiya Akademii Nauk, Teoriya i Sistemy Upravleniya, 2019, No. 5, pp. 117–129.

CONTROL SYSTEMS OF MOVING OBJECTS

Passive System for the Angular Damping of the SAMSAT-QB50 Nanosattelite

I. V. Belokonov[a], D. S. Ivanov[b,*], M. Yu. Ovchinnikov[b], and V. I. Pen'kov[b]

[a] *Samara National Research University, Samara, 443086 Russia*

[b] *Keldysh Institute of Applied Mathematics, Russian Academy of Sciences, Moscow, 125047 Russia*

**e-mail: danilivanovs@gmail.com*

Received March 25, 2019; revised April 29, 2019; accepted May 20, 2019

Abstract—The angular motion of a nanosatellite equipped with a hysteresis damping system is studied. The required number and sizes of hysteresis rods needed to achieve the specified transient time and aerodynamic orientation with a given accuracy are chosen. Laboratory measurements of parameters of the chosen hysteresis rods are presented. The transient time in the case of abnormal launch of the nanosatellite is estimated.

DOI: 10.1134/S1064230719050046

INTRODUCTION

In experiments concerning the study of the upper layers of the atmosphere, it is preferable to orient a satellite so that its longitudinal axis is directed along the vector of incident air flow. The lifetime of such a satellite depends on its shape, mass, and the orbit altitude, but usually it is small and can range from several months to several days. Therefore, increased requirements to the speed of the orientation system are imposed [1, 2].

The defining features of the orientation systems of small satellites are the simplicity of design, low cost, and the absence of energy-consuming elements [3]. Therefore, micro- and nano-class satellites often employ passive orientation systems: magnetic, gravitational, and aerodynamic. As a rule, they include hysteresis dampers in the form of rods that dissipate the energy of the perturbed angular motion of the satellite after separating from the launch vehicle and ensure the asymptotic stability of the motion of the satellite axis. More often, hysteresis rods are used as part of a passive magnetic orientation system, in particular, on nanosatellites Munin (2000) [4], QuakeSat (2003) [5], CUTE-I XI-IV (2003) [6], EduSAT (2011), Delfi-C^3 (2008) [7], TNS-0 No. 1 (2005) [2], and TNS-0 No. 2 (2017) [8]. Less commonly, hysteresis rods are used in passive gravitational and aerodynamic orientation systems for small satellites. For example, it is worth noting the 6-kg REFLECTOR nanosatellite [9] with a gravitational system, put into orbit in 2000, and the MAK-A satellite [3] with a passive aerodynamic orientation system. The development and use of passive orientation systems is of particular interest for universities and small companies entering the market for space services.

In this paper, we consider the SamSat-QB50 nanosatellite [10], which consists of three series-connected cubic parts, the last of which is hollow, as a result of which the center of pressure is offset from the center of mass, which leads to the creation of a recovering aerodynamic moment. To ensure an aerodynamic orientation, it is necessary to damp the initial spin-up after separation from the launch vehicle. This can be done using a set of hysteresis rods. The choice of rods determines the time required to achieve an orbital orientation, which should be sufficiently small, and determines the accuracy of the orientation with respect to the incident flow. In steady motion, the hysteresis rods no longer work as a damper and create a disturbing magnetic moment, which gives rise to undamped forced oscillations about the equilibrium position. Thus, it is necessary to study how the residual magnetic moment of the rods affects the characteristics of steady motion.

For the mathematical modeling of the motion of a satellite equipped with hysteresis rods, it is necessary to know the actual parameters of the hysteresis curve of the rods. The magnetic permeability and the coercive force of the rods determine the damping rate and the residual magnetic moment, which affects the accuracy of its orientation in steady motion. With the help of specialized laboratory equipment available at the Keldysh Institute of Applied Mahematics of the Russian Academy of Sciences (KIAM RAS),

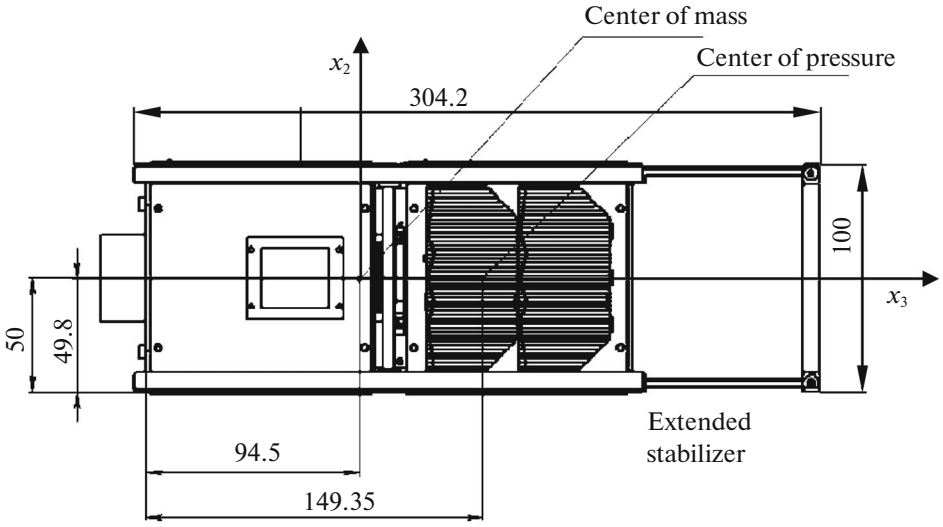

Fig. 1. Drawing the SamSat-QB50 satellite and the axis of the satellite reference frame.

experimental measurements of these parameters of hysteresis rods for the SamSat-QB50 satellite were carried out. This paper presents a method for choosing hysteresis rods to ensure the required transient time for reaching the steady state and achieving the required orientation accuracy of the longitudinal axis of a satellite in the steady state. For the case of an abnormal angular velocity of separation from the launch vehicle, the transient time for reaching the steady state is estimated.

1. SAMSAT-QB50 NANOSATELLITE

The SamSat-QB50 satellite was designed during the participation of the Samara University in the international project QB50 [11] and was designed to monitor the Earth's thermosphere. The satellite is based on the standard CubeSat nanosatellite technology and consists of three 10 × 10 × 10 cm blocks. The SamSat-QB50 nanosatellite is supposed to use a hybrid orientation and stabilization system consisting of an active electromagnetic system for damping the initial angular velocity and a passive aerodynamic system with a hysteresis damper. An aerodynamic moment appears when transforming a 2U cubesat into a 3U cubesat after separation from the launch vehicle. The satellite is transformed by extending a stabilizer consisting of a hollow 1U block, which leads to a shift of its pressure center with respect to the center of mass. The satellite is planned to be launched into a low circumpolar orbit. The mass of the satellite is 1.95 kg, and the inertia tensor in the central axes in kg m^2 is

$$J = \begin{bmatrix} 1.17\times10^{-2} & 0 & 0 \\ 0 & 1.15\times10^{-2} & 0 \\ 0 & 0 & 4.43\times10^{-3} \end{bmatrix}.$$

The coordinates of the pressure center in the satellite reference frame (in mm) are

$$\mathbf{r}_c = \begin{bmatrix} -1.9 \\ 0.2 \\ 54.8 \end{bmatrix}.$$

Dimensional drawings with the position of the center of mass and the center of pressure, as well as the satellite reference frame, are presented in Fig. 1.

2. LABORATORY STUDIES OF HYSTERESIS RODS

2.1. Choice of Hysteresis Rods

Damping with the help of hysteresis rods is carried out due to their magnetization reversal in the Earth's magnetic field: the kinetic energy transforms into thermal energy, which is proportional to the area

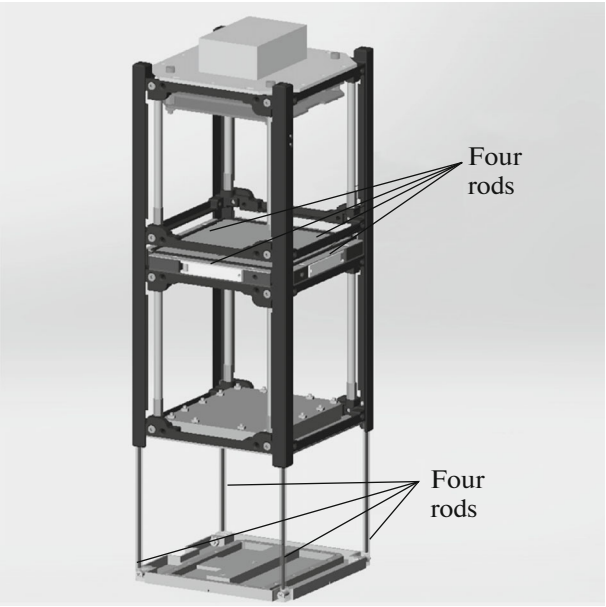

Fig. 2. Arrangement of the hysteresis rods in the satellite body.

of the hysteresis loop. The loop area during magnetization reversal in the Earth's magnetic field depends on the initial permeability μ, equal to the slope of the loop at a zero magnetic field, and on the coercive force H_c, equal to half the width of the loop in a zero magnetic field. The coercive force does not depend on the shape and size of the hysteresis material but the permeability depends on the elongation of the rod: the ratio of its cross section to its length. The greater the elongation of the rods the closer the permeability to the rated value of the material.

For the angular damping system, hysteresis rods were made of 79NM permalloy annealed in a vacuum furnace according to the GOST-10160-75 standard. According to the this GOST standard, the magnetic induction coefficient of this material is $\mu = 180\,000$, the coercive force is $H_c = 1.6$ A/m, and the saturation induction is $B_s = 0.75$ T. However, the rated characteristics of the material can differ significantly from the values for specific hysteresis dampers.

To increase the area of the hysteresis loop, it is necessary to take rods with the maximum elongation (the ratio of its length to the largest transverse size), since such rods will have a smaller demagnetization factor and, therefore, a greater μ. However, the number and the length of the rods are structurally limited by the dimensions of the satellite. It is technologically possible to install only eight rods, and their length should not exceed 80 mm (Fig. 2). To reduce the influence of the residual magnetic moment of the rods on the steady motion, it is reasonable to install orthogonal triples of identical rods, as was done on the MAK-A satellite [3, 12]. Thus, on the SamSat-QB50 satellite, it is possible to place a maximum of two perpendicular triples or six 80-mm long rods. However, six rods may not be enough in terms of the requirements on the time for angular damping after separation and it will be necessary to install a maximum possible number of rods. This will lead to an increase in the residual magnetic moment and, therefore, to an additional perturbation acting on the vehicle in the steady aerodynamic position. This, in turn, will entail an increase in the deviation angle of the vehicle relative to the incident flow, which may be unsatisfactory for the mission. Therefore, the choice of rods is critical both for transient processes and for the motion in the vicinity of the aerodynamically stabilized position.

An important parameter of the rods is their elongation. At a fixed maximum length, the variable parameter is their cross section. If we increase the elongation of the rods (reduce their cross section while maintaining a length of 80 mm), the loop area S_{hist} will increase but the volume will decrease. The total energy loss per cycle of magnetization reversal, E_{loss}, is equal to the product of the volume of all rods, V, and the area of the hysteresis loop, S_{hist}:

$$E_{loss} = S_{hist}V.$$

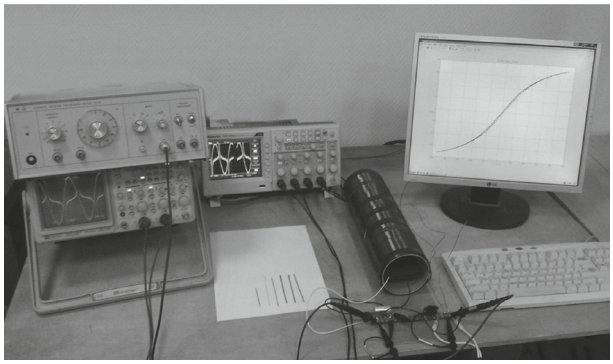

Fig. 3. Laboratory bench for studying the properties of hysteresis dampers.

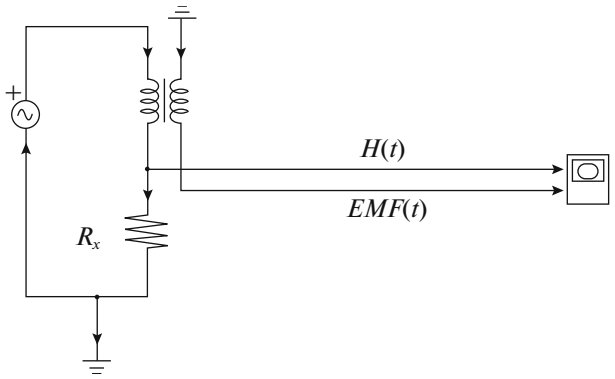

Fig. 4. Schematic of the measurement setup.

Therefore, for different variants of rods, it is necessary to estimate the energy loss during damping in order to achieve damping in the required time at a given initial angular velocity after separation. To correctly estimate the energy loss in the hysteresis rods and estimate the transient time in the satellite's angular motion, it is necessary to have reliable information about their magnetic characteristics. For this purpose, a special laboratory bench is used.

2.2. The Bench for Measuring the Magnetic Characteristics of a Hysteresis Material

The laboratory bench includes a periodic signal generator, a large-diameter coil, a measuring coil, and an oscilloscope (Fig. 3). A change in the voltage across the ends of the large-diameter coil induces an alternating magnetic field into which the test material is placed. The measuring coil is used to determine the magnetic induction inside the hysteresis material. The signal from the generator and the signal from the measuring coil are fed to the digital oscilloscope. The time-base sweep of the received signals is processed using specialized software. The results of processing are used to plot a hysteresis loop of the material, from which the actual coercive force, permeability, and saturation induction—the main parameters characterizing the damping properties of a hysteresis material—are determined. More information about the laboratory bench can be found in [13]. A similar bench is considered in [14] for the study of hysteresis rods for 3U CubeSat of the CSSWE mission with a passive orientation system. The present bench is part of a laboratory at Keldysh Institute of Applied Mathematics, Russian Academy of Sciences (KIAM RAS) in which semi-field studies of the control systems for microsatellites are conducted [15–18].

The experimental hysteresis loop is plotted using the electric circuit shown in Fig. 4. The primary circuit is powered with a voltage source. In the circuit of the primary coil (solenoid), the measuring resistance R_x is series-connected; the voltage across it is proportional to the current and, consequently, to the magnetic field H_e.

The magnetic field inside the solenoid can be represented as

$$H_e = \frac{N_1 I_1}{l_{sol}}.$$

At the input of the second channel of the oscilloscope, we have the signal

$$E_2 = -N_2 \frac{d\Phi}{dt}.$$

Here, $\Phi = BS$ is the magnetic flux, I_1 is the current in the primary coil, N_1 and N_2 are the numbers of turns of the coils, S is the cross-sectional area of the hysteresis sample, B is the magnetic induction inside the rod, l_{sol} is the length of the primary coil, and E_2 is the measured voltage across the secondary coil. From Ohm's law, it follows that $I_1 = E_1/R_x$, where E_2 is the measured voltage at the primary coil. Then, the external field H_e and the magnetic induction B inside the sample can be calculated as follows:

$$H_e = \frac{N_1 E_1}{l_{sol} R_x}, \tag{2.1}$$

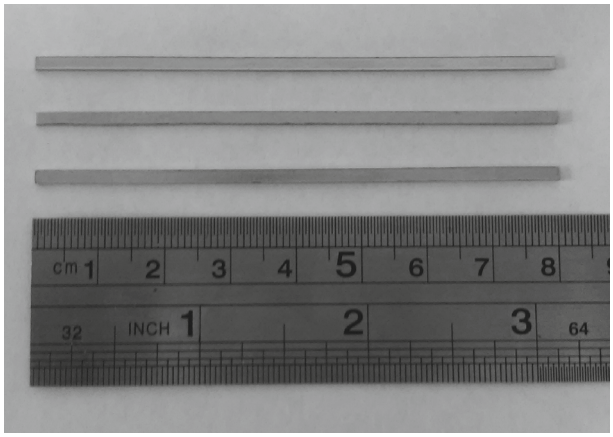

Fig. 5. Hysteresis rods under study.

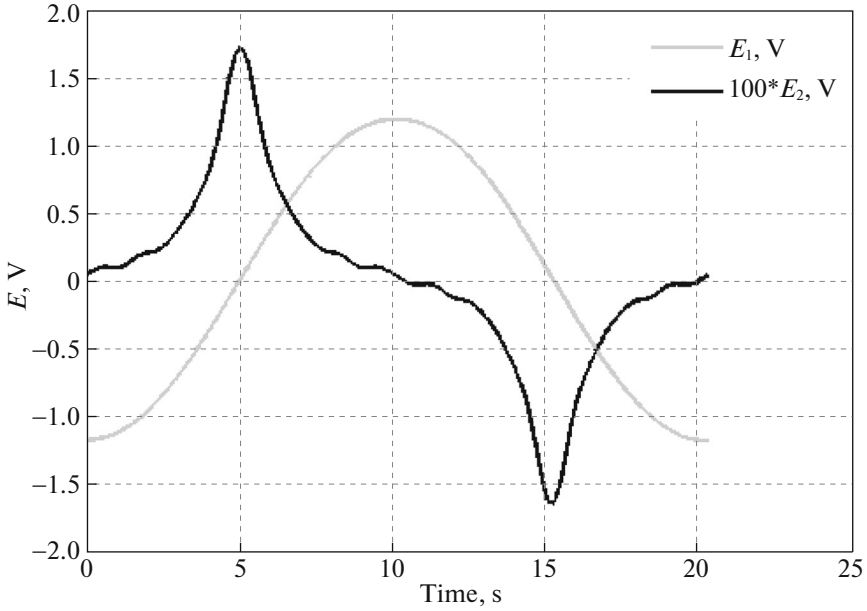

Fig. 6. Signals from external and measuring coils.

$$B = \frac{1}{N_2 S}\int_0^T E_2 dt, \tag{2.2}$$

where T is the time of the voltage measurement across the primary coil.

Thus, from the measurements across the primary and measuring coils, a hysteresis loop of the test material is constructed according to formulas (2.1) and (2.2), from which the characteristics of the material are evaluated.

2.3. Measuring the Parameters of the Hysteresis Loops of Rods

According to the preliminary estimates, hysteresis rods with dimensions of 1 × 2 × 80 mm were chosen (Fig. 5). For these rods, the magnetic characteristics were measured using the laboratory bench described above.

Figure 6 exemplifies the time dependence of the voltages measured across the primary and secondary coils. To smooth the measurements, the first 10 terms of the Fourier series are retained. Next, the pro-

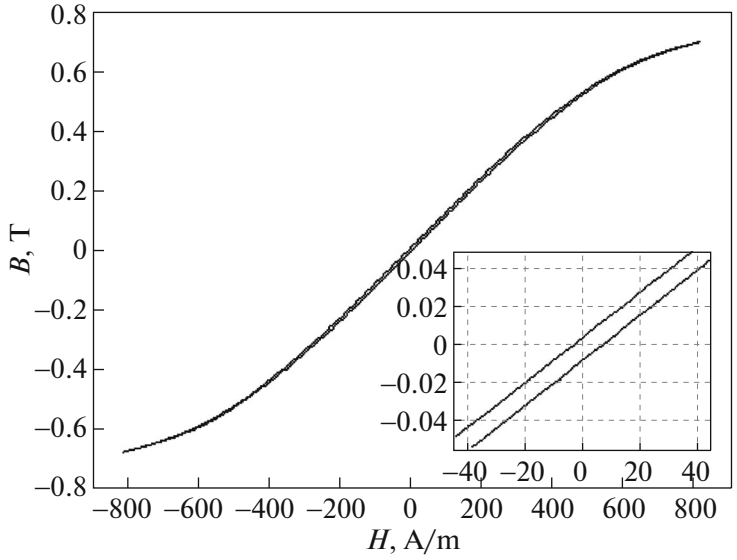

Fig. 7. Resulting hysteresis loop and its increase in the vicinity of zero.

cessed signal from the measuring coil is integrated numerically by the trapezoid method. Formulas (2.1) and (2.2) give H_e and B, respectively.

Figure 7 shows a hysteresis loop for the rods under study, which implies that the permeability is $\mu = 1000 \pm 50$ and the coercive force is $H_c = 3 \pm 1$ A/m.

Now that we have succeeded in measuring the parameters of the hysteresis rods installed in the satellite, we will proceed to the simulation of its transient and steady motion in orbital flight in order to estimate the transient time and the accuracy of aerodynamic stabilization.

3. EQUATIONS OF THE ANGULAR MOTION OF A NANOSATELLITE

Let us consider the motion of a satellite with hysteresis rods of a magnetic material in its body under the action of aerodynamic, gravitational, and magnetic moments. The satellite is a rigid body moving in a circular orbit around the Earth; the Earth's gravitational field is central, Newtonian. The geomagnetic field is approximated by a dipole field located at the center of the Earth parallelly to the rotation axis. To describe the hysteresis in the rods, we use an *improved model* [19]. When calculating the recovering aerodynamic moment, it is assumed that the effect of the atmosphere on the satellite is reduced to the drag force applied at the center of pressure and directed against the velocity of the satellite's center of mass. The density of the atmosphere along the satellite's orbit is assumed to be constant.

The equations of motion of the satellite is written in two right-hand right-angle Cartesian systems. System $Ox_1x_2x_3$ is associated with the satellite. The Ox_3 axis is the longitudinal axis of the satellite. Point O coincides with its center of mass. The other two axes lie in a plane orthogonal to the Ox_3 axis, as shown in Fig. 1. System $OX_1X_2X_3$ is the orbital reference frame. The OX_3 axis is directed along the geocentric radius vector of point O, the OX_2 axis is co-directed with the vector of the orbital kinetic moment, and the OX_1 axis is extended to the right-hand triple.

The position of the satellite reference frame relative to the orbital reference frame is determined using the aircraft's angles α, β, and γ. The elements of the transition matrix $\mathbf{A} = \|a_{ij}\|$ from the orbital to the satellite reference frames are $a_{ij} = \cos(X_i, x_j)$, where $i, j = 1, 2, 3$, and X_i and x_j are the unit vectors of the corresponding axes.

We write the equations of the satellite motion as

$$\mathbf{J}\dot{\boldsymbol{\Omega}} + \boldsymbol{\Omega} \times \mathbf{J}\boldsymbol{\Omega} = \mathbf{M}_a + \mathbf{M}_g + \mathbf{M}_m,$$

$$\dot{\mathbf{A}} = \boldsymbol{\omega} \times \mathbf{A},$$

where $\mathbf{J} = \mathrm{diag}(A, B, C)$ is the diagonal tensor of inertia; $\mathbf{\Omega}$ is the vector of the absolute value of satellite's angular velocity; $\mathbf{M}_a$, $\mathbf{M}_g$, and $\mathbf{M}_m$ are the vectors of the recovering aerodynamic, gravitational, and magnetic moments, respectively; $\boldsymbol{\omega}$ is the vector of the angular velocity of the satellite reference frame relative to the orbital reference frame, which has the form

$$\boldsymbol{\omega} = \mathbf{\Omega} - \mathbf{A}\boldsymbol{\omega}_0,$$

and $\boldsymbol{\omega}_0$ is the angular velocity vector of the orbital motion of the satellite's center of mass, having in the orbital reference frame the form $\boldsymbol{\omega}_0 = \begin{bmatrix}0 & \omega_0 & 0\end{bmatrix}^{\mathrm{T}}$. The gravitational moment in the given case is written as

$$\mathbf{M}_g = 3\omega_0^2 \mathbf{e}_3 \times \mathbf{J}\mathbf{e}_3.$$

Here, $\mathbf{e}_3$ is the unit vector of the axis OX_3, written in the satellite's reference frame.

When modeling the aerodynamic moment, the satellite is assumed to be a parallelepiped composed of six plates. As a result, the moment consists of three moments acting on the three faces facing the incident flow. Let us present an expression for the moment acting on one face of the satellite. Let $\mathbf{n}$ be the vector normal to the face; then, the force acting on the panel in the orbital reference frame is expressed as

$$\mathbf{F}_a = \begin{bmatrix}-\rho S c_x |\mathbf{V}| (\mathbf{n} \cdot \mathbf{A}\mathbf{V}) & 0 & 0\end{bmatrix}^{\mathrm{T}},$$

where ρ is the density of the atmosphere; the velocity vector of the satellite's center of mass, $\mathbf{V} = \begin{bmatrix}\omega_0 r & 0 & 0\end{bmatrix}^{\mathrm{T}}$, is directed against the incident flow; r is the radius of the satellite orbit; S is the area of the face; and c_x is the drag coefficient of the face. The moment of the aerodynamic force relative to the center of mass is

$$\mathbf{M}_a = (-\mathbf{d} + \mathbf{p}) \times \mathbf{A}\mathbf{F}_a.$$

Vector $\mathbf{d}$ specifies the offset of the center of mass of the vehicle relative to the center of pressure, and $\mathbf{p}$ is the vector connecting satellite's center of pressure and the geometric center of the face. To obtain the moment acting on the satellite, it is necessary to sum up three moments for the faces whose normal vectors make an acute angle with the velocity vector of the satellite's center of mass, i.e., $\mathbf{n} \cdot \mathbf{A}\mathbf{V} > 0$.

The rods used have a sufficiently large length-to-diameter ratio; therefore, the magnetic induction vector in the rod is directed practically along its axis and, with an appropriately chosen material, its permeability reaches the desired value. The magnetic moment of the rod can be written as $\mathbf{m} = \mu V_b H_0 W \mathbf{e}/\mu_0$, where μ is the relative permeability of the rod, V_b is its volume, H_0 is the characteristic magnitude of the vector $\mathbf{H}$ of the geomagnetic field at the current point of the orbit, $W(H_\tau)$ is a dimensionless function describing the dependence of the induction of the rod related to H_0 (its specific form is determined by the chosen hysteresis model and, hereinafter, W will be called a hysteresis function), and μ_0 is the magnetic constant; $H_\tau = \mathbf{H}\mathbf{e}$, where $\mathbf{e}$ is the unit vector directed along the rod, written in the satellite reference frame. It should be noted that the main characteristics of the hysteresis loop, the coercive force H_c and saturation induction B_s, are almost independent of the shape of the rod but are determined by its material and heat treatment mode. The relative permeability depends on the magnitude of the magnetizing field H_τ and the elongation of the rod. This fact is explained by the presence of a demagnetizing factor, which decreases with increasing elongation. For the magnitude of the magnetic moment acting on the rod, we have the formula $\mathbf{M}_m = \mathbf{m} \times \mathbf{H}$. If there are several rods installed on the satellite, then, neglecting their mutual influence, the magnetic moment of the entire system can be represented as the sum of the magnetic moments of each rod.

If the satellite has three identical mutually perpendicular rods, then, within the parallelogram hysteresis model, after summing up the expressions describing the magnetic mechanical moment from each rod, only the terms proportional to $k \operatorname{sgn} \dot{H}_\tau$ remain. Such a configuration of rods leads to a reduction in their disturbing effect on the steady motion of the satellite [12].

4. SIMULATING THE ANGULAR MOTION OF THE SATELLITE AFTER LAUNCH

We will conduct a numerical simulation of the angular motion of the SamSat-QB50 satellite in order to choose the number of rods necessary to achieve the required transient time, which should not exceed

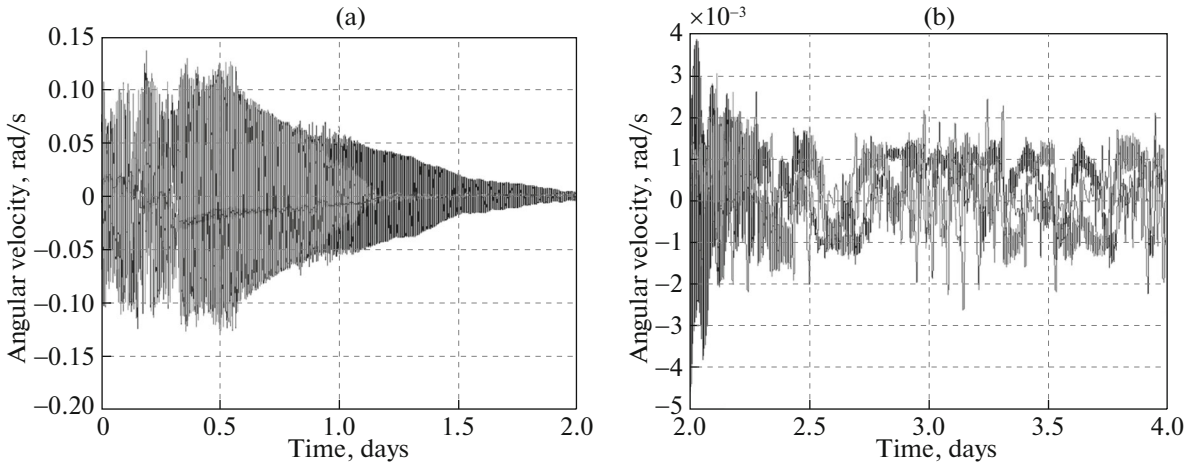

Fig. 8. Angular velocity in the interval (a) from launch to 2 days and (b) from 2 to 4 days. The case of six rods with H_c = 4 A/m.

2 days for the initial longitudinal component of the angular velocity of ±0.1 deg/s and its transverse component of ±0.5 deg/s. In addition, it is necessary to achieve in steady motion an orientation accuracy within ±10° relative to the incident flow vector.

Since the magnitude of the coercive force of the rods has a decisive effect both on the transient time and on the accuracy of steady motion and is experimentally determined with a rather large error $H_c = 3 \pm 1$ A/m, it is reasonable to carry out the simulation with its larger (4 A/m) and smaller (2 A/m) values. If we take the largest possible value, then we should expect a shorter transient time, since the loop will have a larger area and worse accuracy of the steady state due to the residual magnetic moment. In contrast, with the least value, the transient time will be longer but the accuracy of the steady motion higher. Let us consider two configurations of the rods.

4.1. Configuration of Six Rods

We will perform a simulation with two perpendicular triples of hysteresis rods with dimensions of 1 × 2 × 80 mm each. First, we will carry out a simulation for the case of H_c = 4 A/m in order to estimate the maximum damping rate and the worst orientation accuracy. We specify the initial orientation in such a way that the axis of symmetry make an acute angle with the direction of the incident air flow. In this case, the system possesses a potential energy and the aerodynamic moment will spin up the satellite at the initial moment of time, converting the potential energy into kinetic one. Thus, we consider the worst case for the damping system in terms of the initial orientation. We chose for the simulation an orbit with an altitude of 400 km and an inclination of 98°.

Figures 8 and 9 show the time dependences of the components of the angular velocity, and Fig. 10 shows graphs of the deviation of the satellite axis Ox_3 from the incident flow vector. The axes of the satellite reference frame are chosen so that, in the steady state, the angle between the longitudinal axis of the satellite and the velocity vector on the graphs are close to 180°. Figure 9 shows a graph of the angular velocity at the beginning of the simulated motion, which implies that the aerodynamic moment spins up the satellite to an angular velocity of approximately 10 times the initial angular velocity.

It can be seen from the graphs that the transient time, even in the case of a wide hysteresis loop, H_c = 4 A/m, is slightly greater than 2 days; therefore, for a narrow loop, the time will be knowingly longer. The accuracy of steady motion is about 5°. From this numerical example, it follows that six rods are not enough in terms of the transient time, which should not exceed 2 days, but the requirements to the orientation accuracy are satisfied. Let us analyze how these characteristics will change with the addition of two more rods.

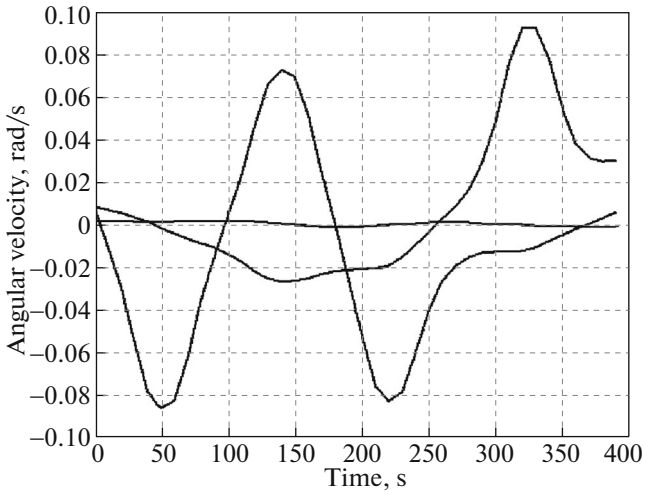

Fig. 9. Angular velocity. Beginning of the motion.

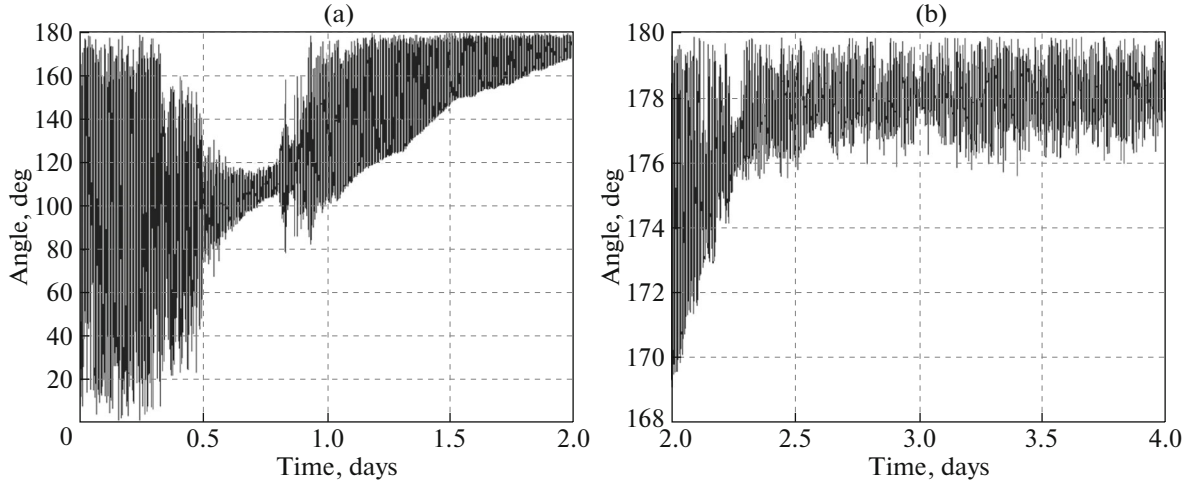

Fig. 10. The angle between the longitudinal axis of the satellite and the velocity vector in the interval (a) from launch to 2 days and (b) from 2 to 4 days. The case of six rods with $H_c = 4$ A/m.

4.2. The Configuration of Eight Rods

Now we study the motion of a satellite with the maximum admissible number of rods: eight rods with dimensions of $1 \times 2 \times 80$ mm each. Note that the addition of two rods along one axis will lead to a reduction in the transient time but will give rise to a disturbing residual magnetic moment, which will affect the accuracy of the steady motion.

First, we will perform a simulation for the case of $H_c = 4$ A/m in order to estimate the maximum damping rate and the worst orientation accuracy. Figure 11 shows the time dependence of the components of the angular velocity, and Fig. 12 shows graphs of the deviation of the satellite axis Ox_3 from the incident flow vector.

It is evident from the figures that the transient time is 1.3 days, which fits into the required 2 days, and the accuracy is about 6°, which is not much worse than in the case of perpendicular triplets of rods and also fits into the required 10°.

Next we simulate the angular motion for the worst case from the point of view of the transient time, $H_c = 2$ A/m. Figure 13 shows the time dependence of the components of the angular velocity, and Fig. 14 shows a graph of the deviation of the satellite's Ox_3 axis from the incident flow vector. It is evident from the figures that the transient time is about 1.7 days and the orientation accuracy in steady state is about 5°. Thus, the configuration of eight rods meets the requirements for the transient time and the accuracy of a steady state.

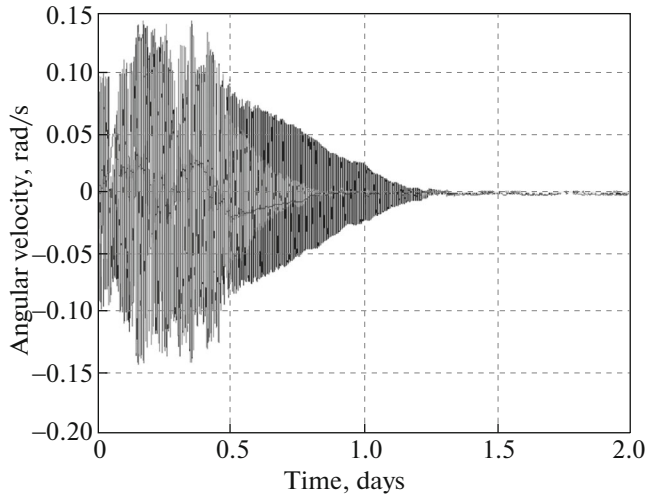

Fig. 11. Angular velocity. The case of eight rods with $H_c = 4$ A/m.

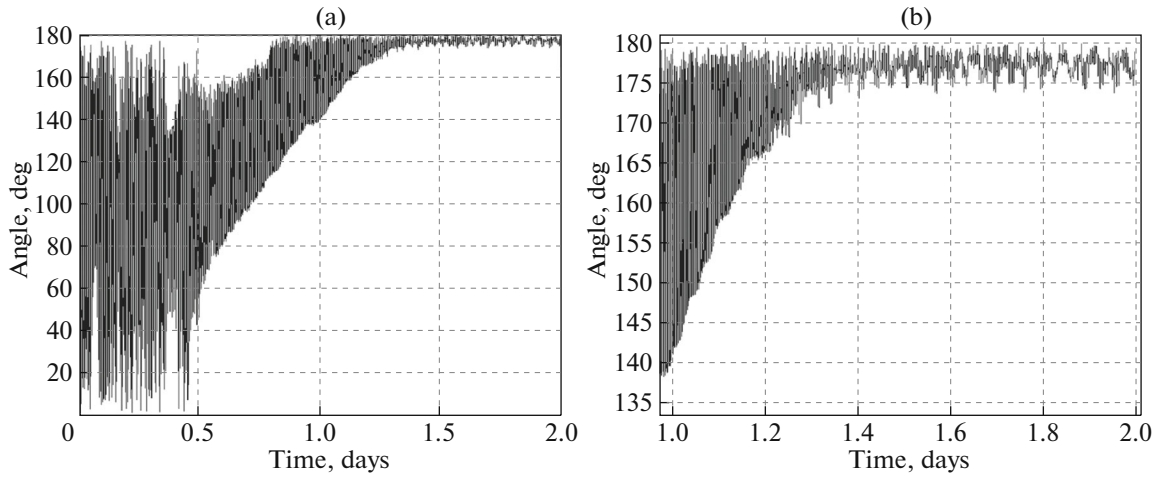

Fig. 12. (a) The angle between the longitudinal axis of the satellite and the velocity vector in the interval from launch to 2 days and (b) the increase in the graph in the interval from 1 to 2 days. The case of eight rods with $H_c = 4$ A/m.

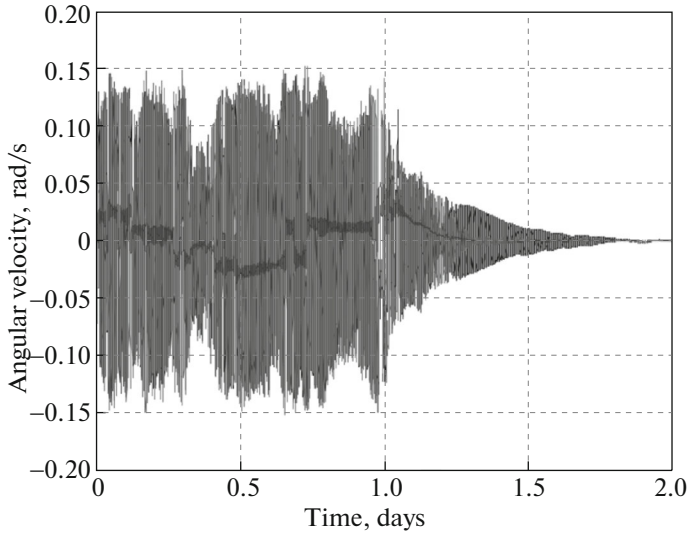

Fig. 13. Angular velocity. The case of eight rods with $H_c = 2$ A/m.

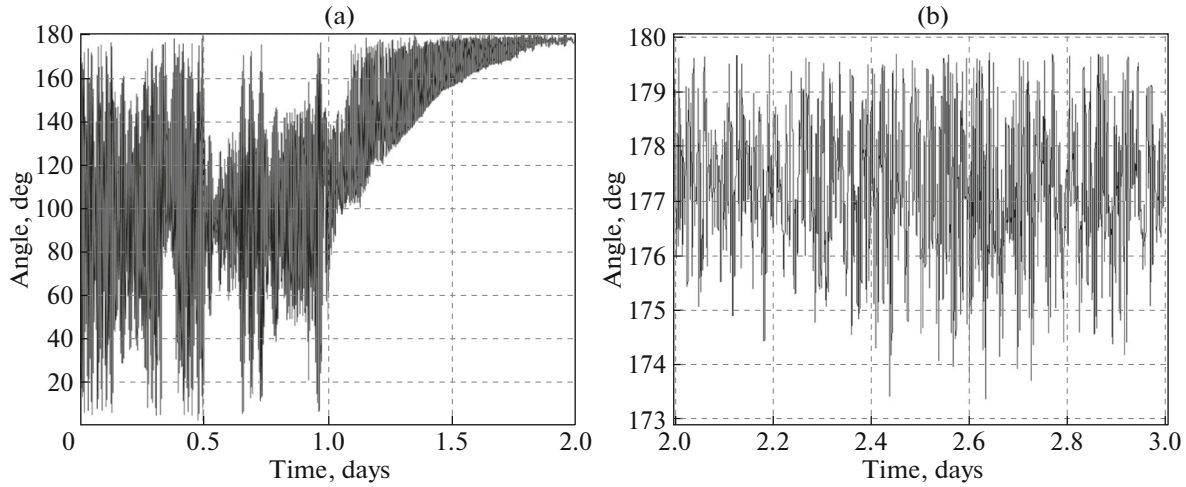

Fig. 14. The angle between the longitudinal axis of the satellite and the velocity vector in the interval (a) from launch to 2 days and (b) from 2 to 3 days. The case of eight rods with $H_c = 2$ A/m.

5. ESTIMATING THE TRANSIENT TIME IN A CONTINGENCY

When launching from a launch barrel, the satellite may acquire an irregular angular velocity much higher than the declared values of 0.5 deg/s. Therefore, it is necessary to preliminary estimate the transient time in the case of installing eight rods with dimensions of $1 \times 2 \times 80$ mm in the case of an abnormal spin-up with an angular velocity, e.g., $\omega_{in} = 50$ and 90 deg/s. From Fig. 7, we can estimate the energy loss during one magnetization reversal of the rods in the Earth's field $H \approx 40$ A/m, equal to the area of the corresponding part of the loop multiplied by the volume of the rod:

$$E_{loss} = S_{hist}V.$$

We take the mean value of the retarding moment equal to

$$M_c = \frac{E_{loss}}{2\pi}.$$

The angular acceleration along one axis can be estimated by the formula

$$\varepsilon = \frac{M_c}{J},$$

where J is the maximum moment of inertia, equal to ≈ 0.0117 kg m^2. For the initial velocity ω_{in}, the transient time can be estimated as

$$t_{fin} = \frac{\omega_0}{\varepsilon}.$$

Table 1 gives an estimate of the transient time for different values of the initial angular velocity and coercive force.

Table 1. Estimated transient time in case of abnormal launch

Considered variant	S_{hist}, T A/m	E_{loss}, J	M_c, N m	$\varepsilon = \frac{M_c}{J}$, rad/s^2	$t_{fin} = \frac{\omega_0}{\varepsilon}$, days
$\omega_0 = 50$ deg/s, $H_c = 2$ A/m	0.12	3.8×10^{-8}	6×10^{-9}	5×10^{-7}	19.8
$\omega_0 = 50$ deg/s, $H_c = 4$ A/m	0.24	7.7×10^{-8}	1.2×10^{-8}	1×10^{-6}	9.9
$\omega_0 = 90$ deg/s, $H_c = 2$ A/m	0.12	3.8×10^{-8}	6×10^{-9}	5×10^{-7}	35.7
$\omega_0 = 90$ deg/s, $H_c = 4$ A/m	0.24	7.7×10^{-8}	1.2×10^{-8}	1×10^{-6}	17.8

Thus, the transient time for the initial angular velocity $\omega_0 = 50$ deg/s may at worst be about 20 days and at best 10 days. For the angular velocity $\omega_0 = 90$ deg/s, the transient time varies from 18 to 36 days.

CONCLUSIONS

As a result of the mathematical modeling of the angular motion of the SamSat-QB50 satellite with hysteresis rods, it has been shown that, in order to meet the requirements to the transient time and the orientation accuracy in steady state, it is necessary to install eight rods with dimensions of $1 \times 2 \times 80$ mm. With an initial angular velocity with a longitudinal component of ± 0.1 deg/s and a transverse component of ± 0.5 deg/s, the damping time ranges from 1.3 to 1.7 days and the orientation accuracy in a steady state is 5°–6°. In the case of a contingency, when the initial angular velocity is 90 deg/s, the transient time can reach 36 days.

REFERENCES

1. M. Yu. Ovchinnikov, V. I. Pen'kov, D. S. Roldugin, et al., *Magnetic Systems of Orientation of Small Satellites* (IPM im. M. V. Keldysha RAN, Moscow, 2016) [in Russian].
2. S. O. Karpenko, N. V. Kupriyanova, M. Yu. Ovchinnikov, et al., "Attitude control system of the first russian nanosatellite TNS-0 No. 1," Cosmic Res. **48**, 517 (2010).
3. V. A. Sarychev and M. Yu. Ovchinnikov, "Aerodynamic orientation system with hysteresis rods," Kosm. Issled. **32** (6), 16–33 (1994).
4. M. L. Battagliere, F. Santoni, M. Ovchinnikov, et al., "Hysteresis rods in the passive magnetic stabilization system for university micro and nanosatellites," in *Proceedings of the 59th IAC, Glasgow, Sept. 29–Oct. 3, 2008,* Paper IAC-08.C.1.8.
5. M. Long, A. Lorenz, G. Rodgers, et al., "A cubesat derived design for a unique academic research mission in earthquake signature detection," in *Proceedings of the 16th Annual/USU Conference on Small Satellites, Aug. 12–15, Logan, Utah, US, 2002,* paper SSC02-IX-6.
6. Y. Tsuda, N. Sako, T. Eishima, et al., "University of Tokyo's CubeSat project – its educational and technological significance," in *Proceedings of the 15th Annual AIAA/USU Conference on Small Satellites, Aug. 13–16, Logan, Utah US, 2001,* paper SSC01-VIIIb-7.
7. F. T. Hennepe, B. T. C. Zandbergen, and R. J. Hamann, "Simulation of the attitude behaviour and available power profile of the Delfi-C3 spacecraft with application of the OpSim platform," in *Proceedings of the 1st CEAS European Air and Space Conference, Sept. 10–13, 2007, Berlin, Germany.*
8. D. S. Ivanov, M. Yu. Ovchinnikov, O. A. Pantsyrnyi, et al., "Angular motion of the TNS-0 nanosatellite No. 2 after launch from the ISS," Cosmic Res. **57** (4) (2019, in press).
9. M. Yu. Ovchinnikov, V. D. Shargorodskii, V. I. Pen'kov, et al., "Nanosatellite REFLECTOR: choice of parameters of the attitude control system," Cosmic Res. **45**, 60 (2007).
10. E. Shakhmatov, I. Belokonov, I. Timbai, et al., "SSAU project of the nanosatellite SamSat-QB50 for monitoring the Earth's thermosphere parameters," Proc. Eng. **104**, 139–146 (2015).
11. QB-50 Project. www.qb50.eu/. Accessed December 1, 2018.
12. V. A. Sarychev, V. I. Pen'kov, M. Yu. Ovchinnikov, et al., "The motion of a gravitational-oriented satellite with hysteresis rods in the plane of the polar orbit," Kosm. Issled. **26**, 654–668 (1988).
13. D. S. Ivanov, M. Yu. Ovchinnikov, and V. I. Pen'kov, "Laboratory study of magnetic properties of hysteresis rods for attitude control systems of minisatellites," J. Comput. Syst. Sci. Int. **52**, 145 (2013).
14. D. T. Gerhardt and S. E. Palo, "Volume magnetization for system-level testing of magnetic materials within small satellites," Acta Astronaut. **127**, 1–12 (2016).
15. D. S. Ivanov, M. Yu. Ovchinnikov, and S. S. Tkachev, "Attitude control of a rigid body suspended by string with the use of ventilator engines," J. Comput. Syst. Sci. Int. **50**, 104 (2011).
16. D. Bindel, I. E. Zaramenskikh, D. S. Ivanov, M. Yu. Ovchinnikov, and N. G. Proncheva, "A laboratory facility for verification of control algorithms for a group of satellites," J. Comput. Syst. Sci. Int. **48**, 779 (2009).
17. D. S. Ivanov, M. D. Koptev, Ya. V. Mashtakov, M. Yu. Ovchinnikov, N. N. Proshunin, S. S. Tkachev, A. I. Fedoseev, and M. O. Shachkov, "Laboratory facility for microsatellite mock-up motion simulation," J. Comput. Syst. Sci. Int. **57**, 115 (2018).
18. D. S. Ivanov, S. O. Karpenko, M. Yu. Ovchinnikov, D. S. Roldugin, and S. S. Tkachev, "Testing of attitude control algorithms for microsatellite 'Chibis-M' at laboratory facility," J. Comput. Syst. Sci. Int. **51**, 106 (2012).
19. V. A. Sarychev, V. I. Pen'kov, and M. Yu. Ovchinnikov, "Mathematical model of hysteresis, based on the magnetic-mechanical analogy," Mat. Model. **1** (4), 122–133 (1989).

Translated by E. Chernokozhin